ORIGINAL ARTICLE

Enantiomeric characterization and structure elucidation of Otamixaban

Jian Shen[a,*], Jiping Yang[a], Winfried Heyse[b], Harald Schweitzer[b], Norbert Nagel[b], Doris Andert[b], Chengyue Zhu[a], Vincent Morrison[a], Gregory A. Nemeth[a], Teng-Man Chen[a], Zhicheng Zhao[a], Timothy A. Ayers[a], Yong-Mi Choi[a]

[a]Sanofi, 1041 Route 202-206, Bridgewater, NJ 08807, United States
[b]Sanofi, Industriepark Hoechst Bldg., D-65926 Frankfurt, Germany

Abstract Otamixaban is a potent (Ki=0.5 nM) fXa inhibitor currently in late-stage clinical development at Sanofi for the management of acute coronary syndrome. Being unproductive in obtaining a suitable crystal of Otamixaban, the required enantiomeric characterization has been accomplished using vibrational circular dichroism (VCD) spectroscopy. Selected by a spectrum similarity index, the calculated spectra of several higher energy conformers were found to match well with the observed spectra. The characteristic IR bands of these conformers were also identified and attributed to the solvation effect. Combined with both the single crystal x-ray diffraction results for an intermediate and the proton NMR study, the absolute configuration of Otamixaban is unambiguously determined to be (R,R).

© 2014 Xi'an Jiaotong University. Production and hosting by Elsevier B.V. All rights reserved.

1. Introduction

As a potent (Ki=0.5 nM) and selective Factor Xa (fXa) inhibitor, Otamixaban is in late-stage clinical development for the management of acute coronary syndrome [1]. Although its stereochemistry was established from the co-crystal structure with fXa [2], the absolute configuration (AC) of Otamixaban from a different synthetic route needs to be verified for both the regulatory requirement and quality control. The task is usually handled by the single crystal x-ray diffraction (scXRD) method [3]. However, our effort to obtain a suitable crystal of Otamixaban was unsuccessful. Since vibrational circular dichroism (VCD) spectroscopy [4–7] is an alternative method

*Corresponding author at: PO Box 112, Readington, NJ 08870, United States. Tel./fax: +1 908 393 1033.
E-mail addresses: jian.shen@simvcd.net, jian-shen@msn.com (J. Shen).

of AC determination, we attempted to explore this approach for Otamixaban.

The VCD method is based on the model-observation agreement. When a simulated spectrum of a model matches the experimental spectrum of a sample, the AC of the model is assigned to the sample. The challenges in Otamixaban AC determination are mainly due to the molecular size and flexibility, which affect both the modeling and experiment. With nine rotational bonds and a molecular weight of 446, Otamixaban is larger and more flexible than most molecules in published VCD studies [8–10]. To simplify the spectrum simulation of large molecules, Dunmire et al. [11] replaced ketoconzole using two small chiral fragments, of 308 and 304 molecular weight. This approximation, however, is not suitable for Otamixaban because its two chiral centers are directly bonded. While today's computing power is capable of the spectrum calculation for the whole Otamixaban, handling the sheer volume of spectrum comparisons and providing the convincing evidence of AC are not trivial.

On the VCD experiment of large and flexible chiral molecules, the band broadening and low signal-to-noise ratio (S/N) were frequently observed due to an increasingly larger number of fundamentals in the VCD sensitive region (1100–1500 cm^{-1}) and multiple populated conformers. As a result, a fewer band-to-band matches can be established between a model and observed spectrum. Because both the conformation and configuration can affect the number and sign of VCD bands, an AC assignment for such a molecule is often questionable without an error estimating.

To overcome the difficulties in the manual spectrum comparison, we [12] developed a VCD spectrum similarity index, S_V, which has been used to select the best matched spectra from calculations. We further discovered that the S_V of unmatched spectra has a normal distribution with a mean value of ~0 and a standard deviation of ~0.1 [13]. This statistical characteristic can

be used to eliminate wrong models and to provide a confidence estimate for an assigned AC. We used the same approach herein for Otamixaban. To provide an unbiased assessment, we assumed no prior knowledge about the chirality of the sample thereby investigating all possible configurations. In addition, IR and NMR were used to study the solution conformations of Otamixaban.

2. Experiment

2.1. Reagents and chemicals

The Otamixaban sample was prepared in our lab through the synthetic route described in Scheme 1.

2.2. IR and VCD data collection and processing

The experimentally observed IR and VCD spectra (4.6 mg Otamixaban dissolved in 0.15 mL DMSO-d_6) were measured by Biotools using ChiralIR-2X with Dual Pem. The spectra were acquired at the resolution of 4 cm^{-1} for 10 h with a path length of 100 μm. The solvent signal was subtracted from both spectra. The measured VCD spectra were corrected for baseline artifacts by subtracting the enantiomer spectra [10]. The conformation search was carried out using Maestro 8.5 (Schrödinger, LLC). In order to save computing resources and to identity the AC quickly, a coarse sampling with an energy cutoff of 5 kcal/mol (20.934 kJ/mol) and an RMSD of 2 Å were used to generate starting conformers for the subsequent density functional theory (DFT) calculations. After eliminating the unmatched stereoisomer, conformation searches with smaller RMSD of 0.5 Å were used to generate additional conformers. Similar to other studies [12,13], Gaussian 03 (Gaussian Inc.) [14] with 6-31G(d) basis set and PBEPBE functional were
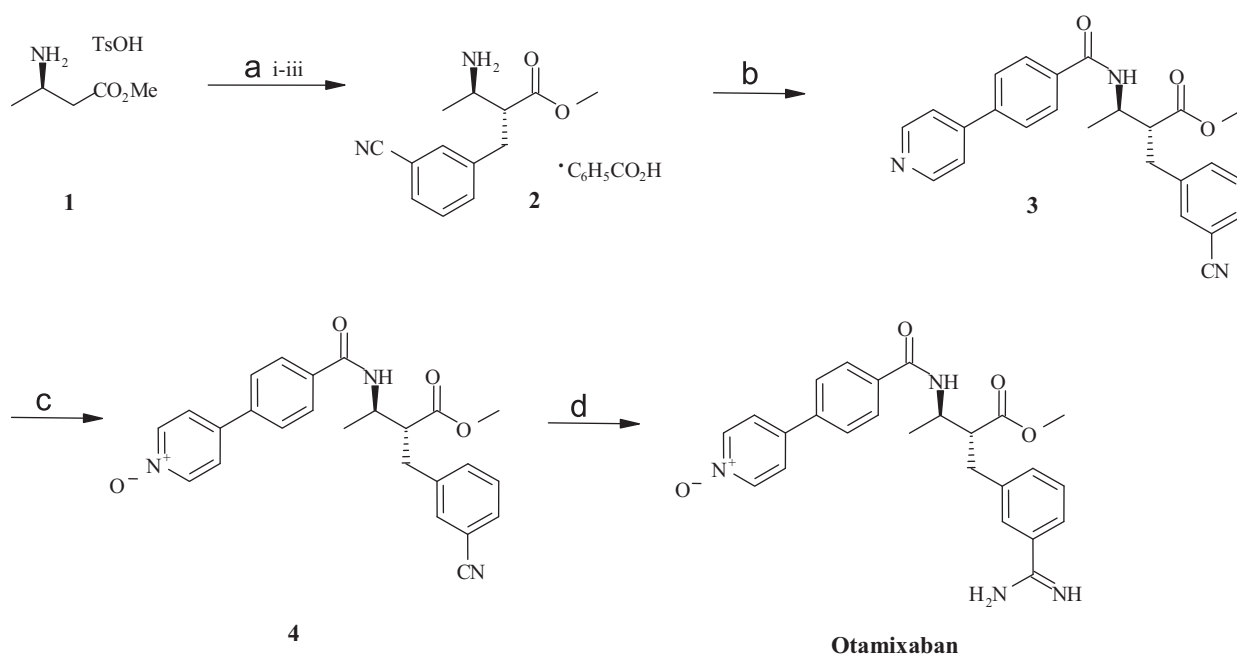
Reagents and conditions: a) i. LiHMDS, THF, −20 °C; ii. 3-cyanobenzylbromide; iii. benzoic acid, water/toluene; b) i. aq. Na_2CO_3; ii. 4-Pyridin-4-yl-benzoic acid; iii. TBTU, NMM, DMF; c) MMPP, CH_2Cl_2/H_2O; d) i. HCl/MeOH; ii. NH_3.

Scheme 1   Synthesis route of Otamixaban.

used for DFT optimization and spectrum calculations. A Lorentzian half-width of 12 cm^{-1} was used to generate the calculated spectra.

The spectrum comparison and alignment were carried out using the SimIR/VCD [12] protocol implemented in Scitegic Pipeline-Pilot 8.0 (Accerys Inc.). Briefly, the two similarities between calculated (c) and observed (o) IR and VCD spectra, respectively, are defined as

$$S_I = \frac{Ico}{Icc + Ioo - Ico} \tag{1}$$

$$S_V = \frac{Ico}{Icc + Ioo - |Ico|} \tag{2}$$

$$I_{ij} = \int Fi(v)Fj(v)\, dv \tag{3}$$

where I_{ij} are the self and overlap integrals of spectra i and j.

The sign of S_V indicates whether the model and the sample have the same AC ($+$) or they are an enantiomeric pair ($-$). The S_I and S_V were either computed directly or optimized in the following procedure. First, the calculated IR spectrum was divided into a number of bands. Each band was then shifted locally to maximize S_I. These optimized shifts were then applied to the calculated VCD spectrum yielding an optimized S_V. For comparison and plotting, the strengths of the measured and calculated spectra were scaled to 0–1 and -1 to 1 for IR and VCD spectra respectively. For conformation averaging, the multiple calculated IR and VCD spectra were added together with the corresponding population weight, and then treated as single spectra in the procedure.

2.3. NMR

The ^{1}H spectra were acquired for an Otamixaban sample ($\sim$4.5 mg dissolved in 0.7 mL of DMSO-d$_6$) on a Varian INOVA 600 MHz NMR spectrometer equipped with a 5-mm cyro-probe. A spectral width of 6225 Hz was used with 16 transients and 8 k data points. The FIDs were zero-filled to 16 k to give a spectral resolution of 0.75 Hz/point. The calculated coupling constants were obtained using MSpin V1.2.1-49 (MestReLab Research S.L) with the Karplus equation [15]

$$^3J = A + B \cos \phi + C \cos 2\phi \tag{4}$$

where ϕ is the dihedral angle with constants A, B and C being 7, -1 and 5, respectively.

2.4. scXRD

Crystallization trials on **4**, the last intermediate of Otamixaban, were executed. One of these trials yielded a crystal (0.5 mm $\times$ 0.08 mm $\times$ 0.04 mm in size) which was investigated on a Bruker/AXS three circle diffractometer, equipped with a SMART APEX area-detector and a copper-K$_\alpha$ microfocus generator. Data frames were collected using the program package SMART V 5.628 (Bruker AXS, 2001) applying ω-scans with step widths of 0.5° and an exposure time of 20 s. Data processing yielded 7624 reflections (ϑ_{min}=2.78, ϑ_{max}=69.20; $-31 < h < 31$, $-5 < k < 4$, $-19 < l < 19$) of which 3080 reflections were unique (R_{int}= 0.0219, R_σ=0.0273). The positions of all H atoms were experimentally determined from a difference Fourier synthesis map, except those bonded to the methoxy group, which were calculated, $S_{goodness\ of\ fit}$=1.028, $R_{all\ data}$=0.0366 ($R_{obs.\ data}$=0.0309 for 2722 reflections with $|F_{obs}| > 4\sigma$, $wR2_{all\ data}$=0.0827, $wR2_{obs.\ data}$=0.0792).

3. Results and discussions

3.1. scXRD

The single crystal structure of intermediate **4** is determined as shown in Fig. 1A. The structure contains disordered oxygen atoms within the carboxyl methyl group with split positions for O01 (O011) and O02 (O021). The site occupancy factors for the disordered atoms were refined to 0.50 for all disordered oxygen atoms (O01, O011, O02, O021). Each molecule in the crystal has two H-bonds (3.072 Å) which connect two neighboring molecules through the amide moiety and form one-dimensional arrays along
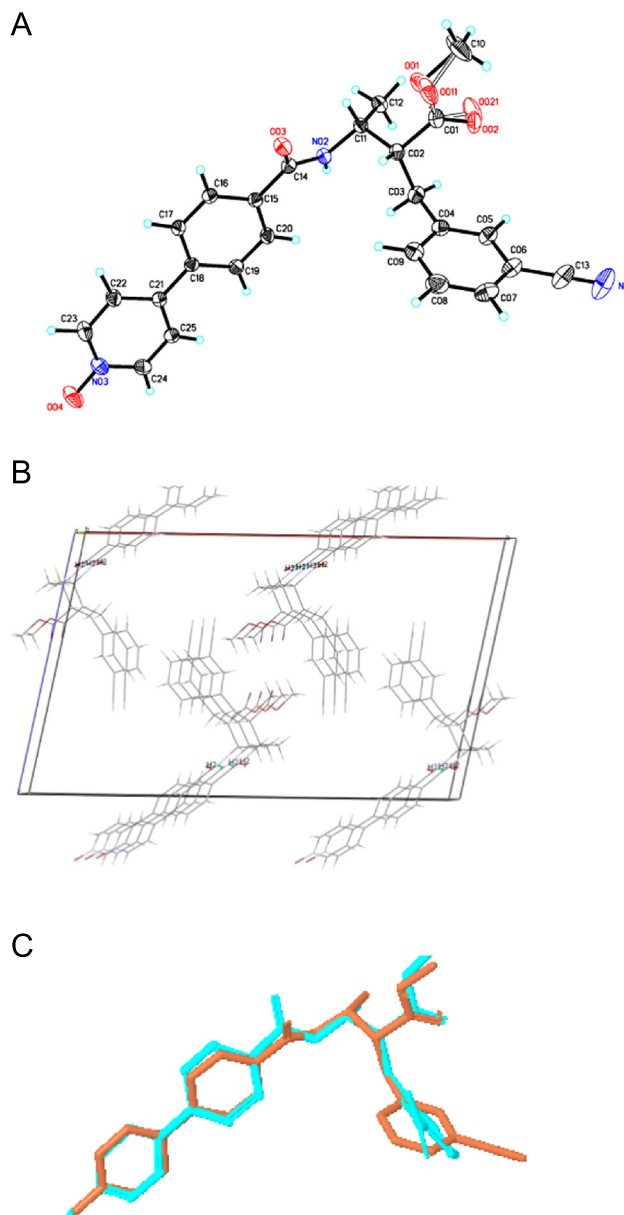

Fig. 1 scXRD structure of Otamixaban intermediate **4**. (A) Molecular structure, atomic numbering scheme and thermal ellipsoids (20%) of the determined molecule; (B) part of the infinite three-dimensional framework; projection nearly along the crystallographic b-axis; hydrogen bonds are given as red and light blue lines; (C) stick models of 4 (orange) and Otamixaban (cyan) in PDB1KNS.

the crystallographic *b*-axis (Fig. 1B). The molecules in each array are closely packed with no space for solvent. There is no observable interaction among the arrays. The overall conformation of the structure is very similar to that of Otamixaban bound to fXa (1 KSN, the ligand was synthesized with a different route) except for the rotation of the 3-phenyl ring as shown in Fig. 1C. The determination of two (*R*) configured chiral centers agrees with the previously determined structure of the intermediate **2** and supports the conclusion that no change of the stereochemistry occurs during the two synthesis steps from **2** to **4**. While this implies a (*R,R*) configuration of the final product, the direct evidence for the Otamixaban's AC is provided by the following VCD investigation.

3.2.   VCD

The experimentally observed VCD spectrum shown in Fig. 2 is not ideal for a straight-forward IR-VCD band-to-band matching. The low signal-to-noise ratio (S/N) gives only a few significant bands as labeled in the VCD spectrum. Among them, bands at 1348.1 cm^{-1} and 1301.8 cm^{-1} appear in a better S/N frequency region. However, their corresponding IR bands are very weak, which makes the IR spectrum less useful for identifying the matching VCD bands in the calculated spectra. It is worth noting that the lower S/N is not unusual as we have seen in other cases of flexible molecules. Although varying experiment conditions might improve the S/N somewhat, the band broadening with reduced signal strength is intrinsic for flexible molecules due to the existence of multiple populated conformations.

The qualitative match between the models and experiment was achieved by statistical analysis; all calculated S_V are shown in
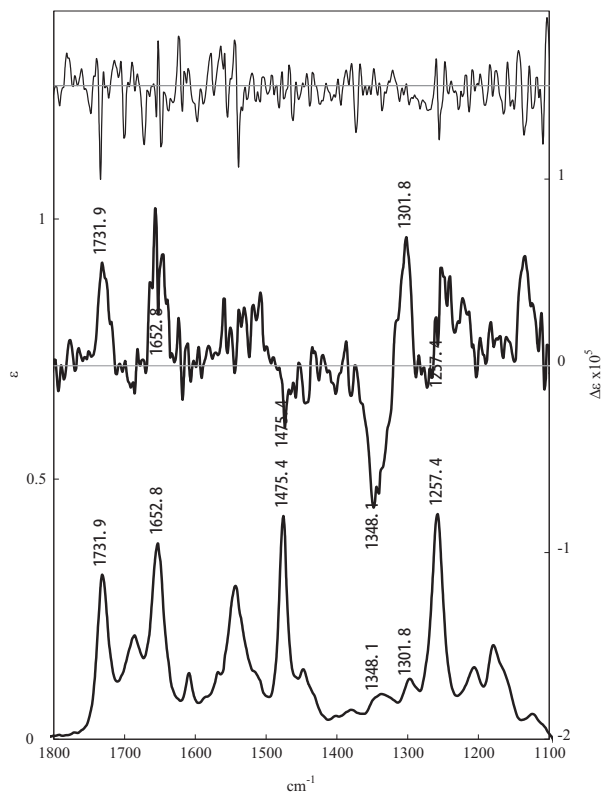

Fig. 2   Observed IR (bottom, left axis), VCD and noise (middle and top with zero baselines, right axis) spectra of Otamixaban in DMSO-d$_6$. The noise spectrum is up-shifted to 1.5 for clarity.

Fig. 3. As Otamixaban has two chiral centers, both (*R,R*) and (*S,R*) stereoisomers were modeled to explore all four possibilities including (*S,S*) and (*R,S*). The S_V of (*S,R*) conformers has a Gaussian-like distribution centered at 0.04 with a standard deviation (SD) of 0.09. No |S_V| was found greater than 0.2 in this group. These characters are similar to those of spectrum-unfit (SU) conformers [13], which implies that (*S,R*) or (*R,S*) is not the AC of the sample.

In contrast, the S_V distribution of (*R,R*) conformers significantly shifts away from zero, with a mean value of 0.14 and an SD of 0.1, which is a sign of spectrum-fit (SF) conformers [13]. Among the (*R,R*) conformers, three are of a higher |S_V| exceeding 0.2, indicating they are likely to be the SF conformers. The VCD spectra of four high S_V conformers (RR2, RR5, RR10, and RR13) were individually aligned with the observed spectrum shown in Fig. 4. The resemblance between the observation and the simulated spectra is apparent. The corresponding values of S_I, and optimized S_V in Table 1 are in the range for matched spectra.

The previous study [13] suggests that properly averaged spectra of SF conformers should yield better agreement with the observation. Indeed, the averaging of the above four spectra improved the optimized S_V to 0.42, which is significantly higher than those of individual spectra. Apparently, the averaged spectrum, ⟨RR⟩, in Fig. 4 resembles the observation better than any individual one. For the averaged IR spectrum, the band at 1525 cm^{-1} appears corresponding to the observed band at 1540 cm^{-1}. There is no observed band corresponding to the calculated band at 1360 cm^{-1}. Given the approximations in calculation and the size and flexibility of the molecule, the calculated spectrum agrees reasonably well with the observed one.

The quantitative AC assessment of Otamixaban is based on the value of optimized S_V [13]. The positive sign of S_V indicates that the ⟨RR⟩ model and the sample are of the same AC. The absolute value of S_V (0.42) is about four times the SD (~0.1). Accordingly, the (*R,R*) assignment of Otamixaban has a confidence level greater than 99.8%. This assignment is consistent with the expectation and the scXRD structure of the final intermediate **4**.

While a VCD spectrum associated with the lowest energy conformer often closely resembles the observed one or weights substantially in conformational averaging, we found this is not the case for Otamixaban. The similarity between the observed spectrum and that of the lowest energy conformer (RR1) is very low with an S_V of 0.09 as shown in Fig. 4 and Table 1. An independent AC confidence assessment using the CompareVOA program [16] for RR1 gave only 52%, much lower than 86% for RR5. Including the RR1 spectrum in averaging with various weights lowered the averaged S_V, indicating that RR1 is not an SF conformer. Obviously, despite its lower energy, RR1 is not significantly populated in the sample based on the spectrum fitness.

We further found that the lower energy of RR1 is caused by an intramolecular H-bond between the amide oxygen and one of benzamidine nitrogen ($d_{O-N}=3.02$ Å). This H-bond also exists in RR2 ($d_{O-N}=3.03$ Å), the second lowest energy conformer, but not in the other three conformers (see Fig. 5). It is well known that polar solvents can weaken intramolecular H-bonds. Although this could explain the mismatch of the RR1 spectrum, we speculated as to whether or not higher energy SF conformers such as RR5 could be detected by other experiments.

The presence of non-H-bond conformers is evident in the 1650–1750 cm^{-1} region of the IR spectrum, which has three major absorption bands corresponding to the NH$_2$ bending (fundamental
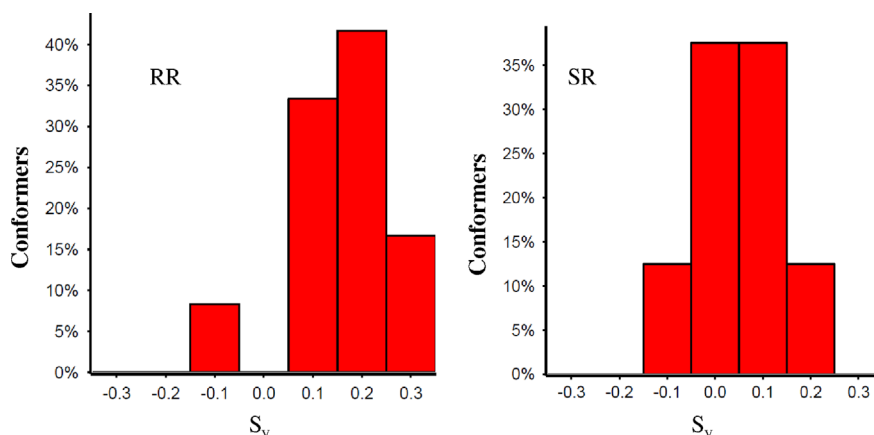
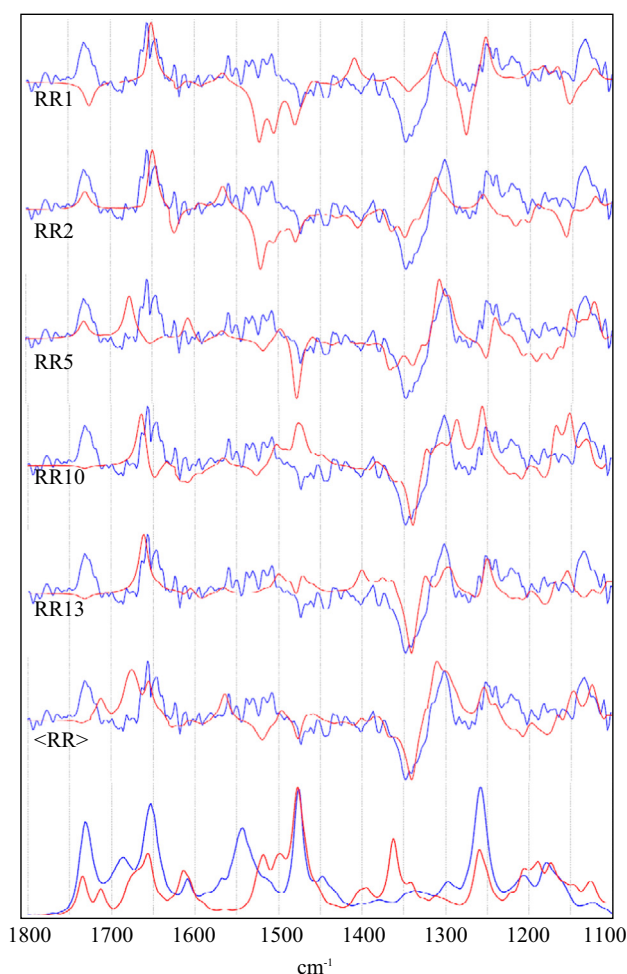Fig. 3   The distribution of S_V for RR and SR conformers.

Fig. 4   The ligned VCD (top 6) and IR spectra of Otamixaban conformers with blue for the experiment and red for the calculation.

143), the C=O stretching of the amide (fundamental 144) and the C=O stretching of the ester (fundamental 145) (see Table 2). For RR1 and RR2, the former two bands are separated by less than 10 cm^{-1} thereby merging into one band in the simulated spectra. In contrast, the IR spectrum of RR5 clearly shows the three distinct bands, which matches the experiment very well. The frequency of fundamental 144 of RR5 is 16–17 cm^{-1} higher than

those of RR1 and RR2. This high frequency shift is also observed in the calculated IR spectra of RR10 and RR13. Both conformers lack the intramolecular H-bond. The C=O band shift in DMSO has been well documented and is attributed to the weakening of the intramolecular H-bond by DMSO-d$_6$ [17].

3.3.   NMR

A common feature of the four SF conformers is their folded conformations with relatively smaller solvent assessable surface area compared with that of the two x-ray structures, shown in Table 1. This seems associated with the values of torsion angle connecting the chiral centers. Is the conformation difference between VCD and x-ray conformers due to the polarity of solvents? In order to answer this question, ^{1}H NMR was applied to the same sample. While the technique cannot detect individual conformation, it can provide information for an averaged torsion angle by measuring the vicinal proton–proton coupling constant ($^3J_{HH}$).

We investigated the torsion associated with the two protons, H_a and H_b, attached to the two chiral carbons. The full ^{1}H NMR spectrum and detailed chemical shifts in Fig. 6 show that $^3J_{HaHb}$ increases from 5.8 in pure DMSO-d$_6$ up to 6.4 with 6% of D$_2$O added. The calculated $^3J_{HaHb}$ values of the four SF conformers shown in Table 1 agree well with the observed value in pure DMSO-d$_6$. In contrast, the calculated $^3J_{HaHb}$ values of the two x-ray conformers closely match the value observed in DMSO-d$_6$ with 6% D$_2$O. Although the empirical prediction depends on a particular set of parameters and can have statistical errors [18], the conformation shifting from pure DMSO-d$_6$ to more polar water-containing solvent has been confirmed. The solvation not only explains the conformation difference between the VCD conformers and x-ray conformers, but also answers why RR1 is not populated in the sample despite its lowest energy from the gas phase calculation.

3.4.   Conformer population

The unfit of RR1 spectrum implies that Boltzmann weighting is not valid for spectrum averaging of Otamixaban models. The equal weighting of the conformer population in this study is based on the spectrum fitness measured by the maximal S_V. We tried to vary individual populations in the spectrum averaging, but no

Table 1   Calculated properties of VCD and x-ray conformers.

Conformer	Energy (kcal/mol)[a]	S_I	S_V	H_a–C–C–H_b torsion (deg)	Calculated $^3J_{HaHb}$ (Hz)	SASA[b] ($Å^2$)
RR1	0	0.61	0.09	−66	5.7	728
RR2	1.93	0.57	0.18	−77	5.1	688
RR5	5.00	0.56	0.30	−73	5.3	695
RR10	12.73	0.76	0.26	69	5.5	696
RR13	13.50	0.73	0.33	68	5.6	690
x[c]	7.41	0.50	−0.09	58	6.4	758
1KSN	6.77	0.65	0.08	54	6.7	725

[a]Relative to DFT energy −1486.42705 Hartree of RR1.
[b]Solvent accessible surface area as calculated with Maestro 8.5.
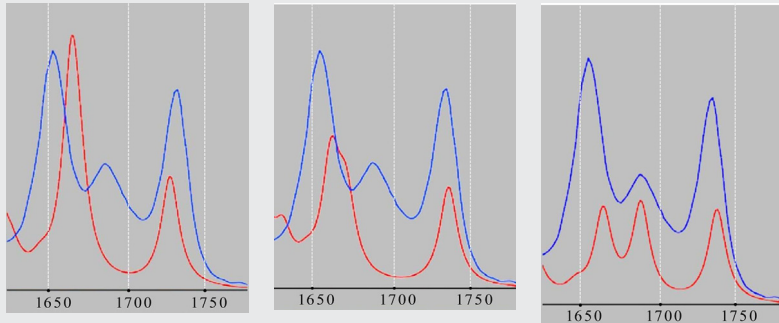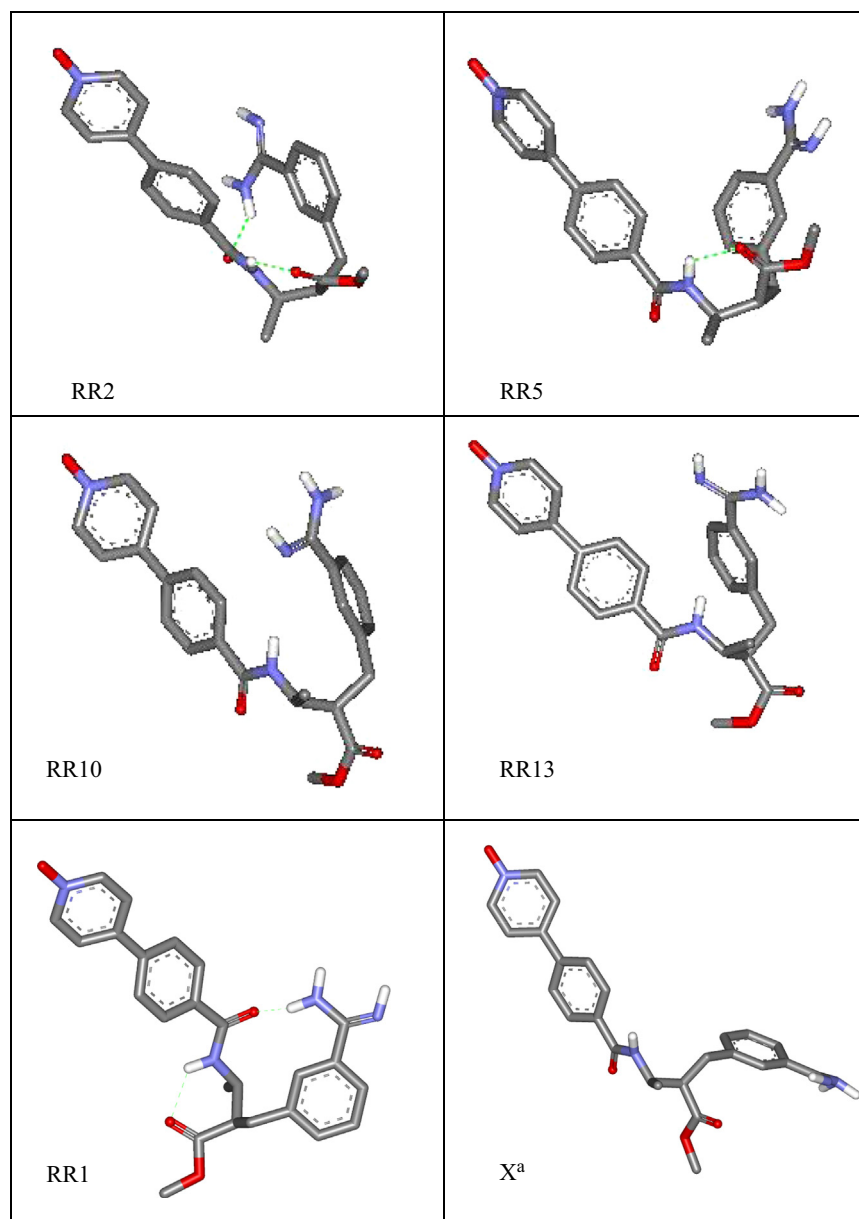[c]Modeled based on the intermediate **4** determined by scXRD in this study.

Fig. 5   The stick model of Otamixaban conformers. [a]Modeled based on the intermediate **4** determined by scXRD in this study. Carbon, oxygen, nitrogen and hydrogen atoms are colored in gray, red, blue and white, respectively. The green dash lines indicate the intramolecular H-bonds. Non-polar hydrogens were removed for clarity.

Table 2   IR frequencies of three bands at high wave number region (cm^{-1}).

Fundamental	RR1	RR2	RR5	Experiment
143	1665	1660	1662	1653
144	1670	1669	1686	1686
145	1727	1733	1735	1732
Spectrum (red)				Blue curves in the left panels
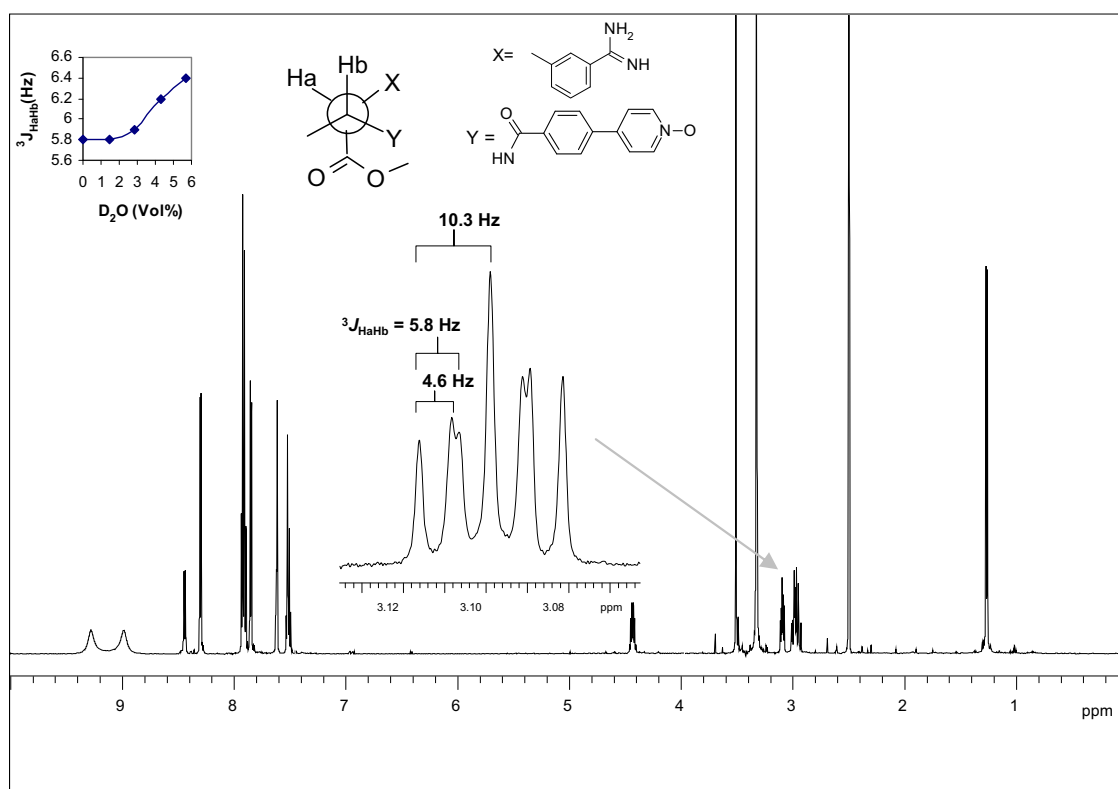
Fig. 6 ^{1}H NMR spectrum of Otamixaban in DMSO-d$_6$. The chemical shifts of H_a and H_b are 3.01 ppm and 4.44 ppm, respectively. The coupling constant $^3J_{HaHb}$ was determined with a varied amount of D$_2$O as shown in the insert.

significant improvement was achieved. This echoes the adjusted population done by Zhang and Polavarapu [19]. They concluded that the conformation averaging with DFT Gibbs energies weighting simply cannot match the experimental results in DMSO-d$_6$. While the use of DFT energy for a conformer in non-polar solvents may be a good approximation, polar solvents, such as DMSO and water, interact strongly with a polar molecule thereby perturbing its energies. In principle, the conformer energies calculated with solvents should be more relevant in the conformer population analysis. However, approaches using either implicit or explicit solvents [20] in VCD calculations generated very limited success

and have not been used widely, especially in industrial research and development. Alternatively, our approach ignores the calculated energies and relies entirely on the compatibility of fit between the calculated and observed spectra, which is a quick yet reliable solution.

Each solution conformer elucidated from the VCD should be considered as a cluster of conformers with smaller structural deviations. For example, the conformation space of the pyridinyl–benzamide can have at least six local minimums by optimizing the two torsions associated with the benzene ring. Because the small variations (<1 Å RMSD) are not directly associated with the chiral

centers, they do not cause significant changes in the calculated VCD spectra. Indeed, the differences of S_V among the subset of RR5 are less than 0.02.

Another structural variation investigated is the tautomerization of the neutral amidine of Otamixaban. Although the amidine is not near to the chiral centers, the energies as well as the spectra vary significantly for different tautomers (see S_I). The current model, e.g. RR5, gives a far better match in the spectrum comparison. Therefore, the other tautomers were ignored.

As we demonstrated, VCD not only gives reliable AC of chiral molecules but also provides rich information about solution structures. Despite many advantages of VCD, scXRD is usually the first option for AC determination. Besides less availability of high performance VCD instrumentation, spectrum calculation and comparison for flexible molecules are often challenging. For molecules like Otamixaban, the number of conformers, including tautomers, can exceed 200 with a finer RMSD cutoff of 0.5 Å. Finding a set of SF conformers (not necessarily the lower energy conformers) requires both computing power and a good spectrum comparison algorithm. As the technology improves, we expect more successful VCD applications to be used for a wide range of chiral molecules. The structures elucidated from VCD experiments will also help us to better understand the solute energy landscape and to improve the force fields and models in molecular modeling and simulations.

4. Conclusion

With the aid of an automated spectrum comparison, the AC of Otamixaban from the large scale synthesis has been unambiguously determined to be (R,R) using VCD. Both visual examination and spectrum similarity comparison indicate that the lowest energy conformer is not populated in DMSO solution. The existence of populated higher energy conformers is confirmed by the characteristic bands in observed and calculated IR spectra. The four leading conformers elucidated in VCD adopt folded conformations with smaller solvent accessible surface area, which differ from the x-ray structures. The NMR study suggests that the conformation difference is due to different solvation environments. For a sizable and flexible pharmaceutical molecule, the spectrum comparison method SimIR/VCD can deliver a consistent performance in finding the best matched spectra from the calculation.

Acknowledgments

Appendix A.   Supplementary material

Supplementary data associated with this article can be found in the online version at http://dx.doi.org/10.1016/j.jpha.2013.10.001.

References

[1] K.R. Guertin, Y.-M. Choi, The discovery of the Factor Xa inhibitor Otamixaban: from lead identification to clinical development, Curr. Med. Chem. 14 (2007) 2471–2481.

[2] K.R. Guertin, C.J. Gardner, S.I. Klein, et al., Optimization of the [beta]-Aminoester class of factor Xa inhibitors part 2: identification of FXV673 as a potent and selective inhibitor with excellent In vivo anticoagulant activity, Bioorg. Med. Chem. Lett. 12 (2002) 1671–1674.

[3] S. Datta, D.J.W. Grant, Crystal structures of drugs: advances in determination, prediction and engineering, Nat. Rev. Drug Discov. 3 (2004) 42–57.

[4] R.D. Shah, L.A. Nafie, Spectroscopic methods for determining enantiomeric purity and absolute configuration in chiral pharmaceutical molecules, Curr. Opin. Drug Discov. Dev. 4 (2001) 764–775.

[5] P.J. Stephens, F.J. Devlin, J.J. Pan, The determination of the absolute configurations of chiral molecules using vibrational circular dichroism (VCD) spectroscopy, Chirality 20 (2008) 643–663.

[6] T.B. Freedman, X. Cao, R.K. Dukor, et al., Absolute configuration determination of chiral molecules in the solution state using vibrational circular dichroism, Chirality 15 (2003) 743–758.

[7] V. Nicu, J. Neugebauer, S. Wolff, et al., A vibrational circular dichroism implementation within a Slater-type-orbital based density functional framework and its application to hexa- and hepta-helicenes, Theor. Chem. Acc.: Theory, Comput. Model. (Theor. Chim. Acta) 119 (2008) 245–263.

[8] M. Urbanová, V. Setnička, P. Bouř, et al., Vibrational circular dichroism spectroscopy study of paroxetine and femoxetine precursors, Biopolymers 67 (2002) 298–301.

[9] O. McConnell, Y. He, L. Nogle, et al., Application of chiral technology in a pharmaceutical company. Enantiomeric separation and spectroscopic studies of key asymmetric intermediates using a combination of techniques, Chirality 19 (2007) 716–730.

[10] D.J. Minick, R.C.B. Copley, J.R. Szewczyk, et al., An investigation of the absolute configuration of the potent histamine H3 receptor antagonist GT-2331 using vibrational circular dichroism, Chirality 19 (2007) 731–740.

[11] D. Dunmire, T.B. Freedman, L.A. Nafie, et al., Determination of the absolute configuration and solution conformation of the antifungal agents ketoconazole, itraconazole, and miconazole with vibrational circular dichroism, Chirality 17 (2005) S101–S108.

[12] J. Shen, C. Zhu, S. Reiling, et al., A novel computational method for comparing vibrational circular dichroism spectra, Spectrochim. Acta Part A: Mol. Biomol. Spectrosc. 76 (2010) 418–422.

[13] J. Shen, Y. Li, R. Vaz, et al., Revisiting vibrational circular dichroism spectra of (S)-(+)-carvone and (1S,2R,5S)-(+)-menthol using SimIR/VCD method, J. Chem. Theory Comput. 8 (2012) 2762–2768.

[14] M.J. Frisch, G.W. Trucks, H.B. Schlegel, et al., Gaussian 03, Gaussian, Inc., Wallingford, CT, 2003.

[15] H. Gunther, NMR Spectroscopy, John Wiley & Sons, Chichester, 1995 (581 pp).

[16] E. Debie, E. De Gussem, R.K. Dukor, et al., Confidence level algorithm for the determination of absolute configuration using vibrational circular dichroism or raman optical activity, ChemPhysChem 12 (2011) 1542–1549.

[17] E. Vass, M. Hollósi, F. Besson, et al., Vibrational spectroscopic detection of beta- and gamma-turns in synthetic and natural peptides and proteins, Chem. Rev. 103 (2003) 1917–1954.

[18] E. Ōsawa, T. Ouchi, N. Saito, et al., Critical evaluation of an empirically modified Karplus equation, Magn. Reson. Chem. 30 (1992) 1104–1110.

[19] P. Zhang, P.L. Polavarapu, Spectroscopic investigation of the structures of dialkyl tartrates and their cyclodextrin complexes, J. Phys. Chem. A 111 (2007) 858–871.

[20] V.P. Nicu, J. Neugebauer, E.J. Baerends, Effects of complex formation on vibrational circular dichroism spectra, J. Phys. Chem. A 112 (2008) 6978–6991.